

Deep Learning-Enabled Text Semantic Communication under Interference: An Empirical Study

Tilahun M. Getu, *Member, IEEE*, Georges Kaddoum, *Senior Member, IEEE*, and Mehdi Bennis, *Fellow, IEEE*

Abstract—At the confluence of 6G, deep learning (DL), and natural language processing (NLP), DL-enabled text semantic communication (SemCom) has emerged as a 6G enabler by promising to minimize bandwidth consumption, transmission delay, and power usage. Among text SemCom techniques, *DeepSC* is a popular scheme that leverages advancements in DL and NLP to reliably transmit semantic information in low signal-to-noise ratio (SNR) regimes. To understand the fundamental limits of such a transmission paradigm, our recently developed theory [1] predicted the performance limits of DeepSC under radio frequency interference (RFI). Although these limits were corroborated by simulations, trained deep networks can defy classical statistical wisdom, and hence extensive computer experiments are needed to validate our theory. Accordingly, this empirical work follows concerning the training and testing of DeepSC using the proceedings of the European Parliament (Europarl) dataset. Employing training, validation, and testing sets *tokenized and vectorized* from Europarl, we train the DeepSC architecture in Keras 2.9 with TensorFlow 2.9 as a backend and test it under Gaussian multi-interferer RFI received over Rayleigh fading channels. Validating our theory, the testing results corroborate that DeepSC produces semantically irrelevant sentences as the number of Gaussian RFI emitters gets very large. Therefore, a fundamental 6G design paradigm for *interference-resistant and robust SemCom* (IR^2 SemCom) is needed.

Index Terms—6G, DL, NLP, SemCom, DL training and testing, IR^2 SemCom.

I. INTRODUCTION

Over the last decade, deep learning (DL) [2] has been propelling the rise of artificial intelligence (AI) [3], in general, and machine learning (ML), in particular. In this remarkable AI/ML era, DL has led to numerous breakthroughs in almost all fields of science, technology, and engineering. Predominantly, DL has led to numerous remarkable results in many fields of computer science, such as image recognition [4], object detection [5], speech processing and recognition [6], and natural language processing (NLP) [7], [8], to mention a few. Due to the rise of DL in NLP, remarkably, statistical

machine translation (SMT) has largely been superseded by neural machine translation (NMT) [9].

On the other hand, DL has spawned depth and breadth of sixth-generation (6G) research [10]–[13] toward ultra-reliable ubiquitous communication, networking, and sensing [14]. With a potential to materialize such 6G services, DL-enabled semantic communication (SemCom) [15]–[17] has arisen to realize the Weaver’s 1949 vision (see [18, Ch. 1]) of a *meaning-centric* communication while promising to minimize transmission delay, bandwidth consumption, and power usage. Driven by these promising prospects, DL has spurred the development of many DL-enabled SemCom techniques in text [15], speech [19], image [20], and video [21] domains. Among the existing text SemCom techniques [16], *DeepSC* is a popular SemCom technique which has enabled the reliable transmission of semantic information in low signal-to-noise ratio (SNR) regimes. However, DeepSC can be severely impacted by *semantic noise* caused by radio frequency interference (RFI) from one or more RFI emitters [1]. In this vein, the performance quantification of DeepSC under interference is crucial to facilitate the design of *interference-resistant and robust* (IR^2) *SemCom systems* [1].

Toward IR^2 SemCom systems, our recent work in [1] has revealed the fundamental asymptotic performance limits of DeepSC. By introducing a principled probabilistic framework, we have shown that – among other limits – DeepSC produces *semantically irrelevant* sentences when all RFI emitters, rendering multi-interferer RFI (MI RFI) [22], get strong and the number of RFI emitters becomes enormous. These performance limits were corroborated by extensive Monte Carlo simulations. Despite the clear-cut theory and corroborating simulations of [1], trained deep networks – such as the DeepSC network – can defy classical statistical wisdom [23]–[26]. Accordingly, extensive computer experiments are needed to verify the performance limits predicted by our recently developed theory in [1]. Apart from the need to validate a theory, there is *no work*¹ thus far – as documented in our survey in [16] – that has studied the impact of interference on text SemCom systems. This dully justifies the need and our motivation for this paper.

In line with the above-highlighted motivation and need, this

¹To the best of our knowledge, there is no work that has empirically investigated the impact of interference on a text SemCom system. However, the authors of [27] studied the impact of semantic noise (due to a malicious attacker) on an image SemCom system and the authors of [28] investigated the impact of wireless attacks, also on an image SemCom system.

T. M. Getu is with the Electrical Engineering Department, École de Technologie Supérieure (ETS), Montréal, QC H3C 1K3, Canada (e-mail: tilahun-melkamu.getu.1@ens.etsmtl.ca).

G. Kaddoum is with the Electrical Engineering Department, École de Technologie Supérieure (ETS), Montréal, QC H3C 1K3, Canada, and the Cyber Security Systems and Applied AI Research Center, Lebanese American University, Beirut, Lebanon (e-mail: georges.kaddoum@etsmtl.ca).

M. Bennis is with the Centre for Wireless Communications, University of Oulu, 90570 Oulu, Finland (e-mail: mehdi.bennis@oulu.fi).

The prior research that has inspired this work was supported by the U.S. Department of Commerce and its agency NIST.

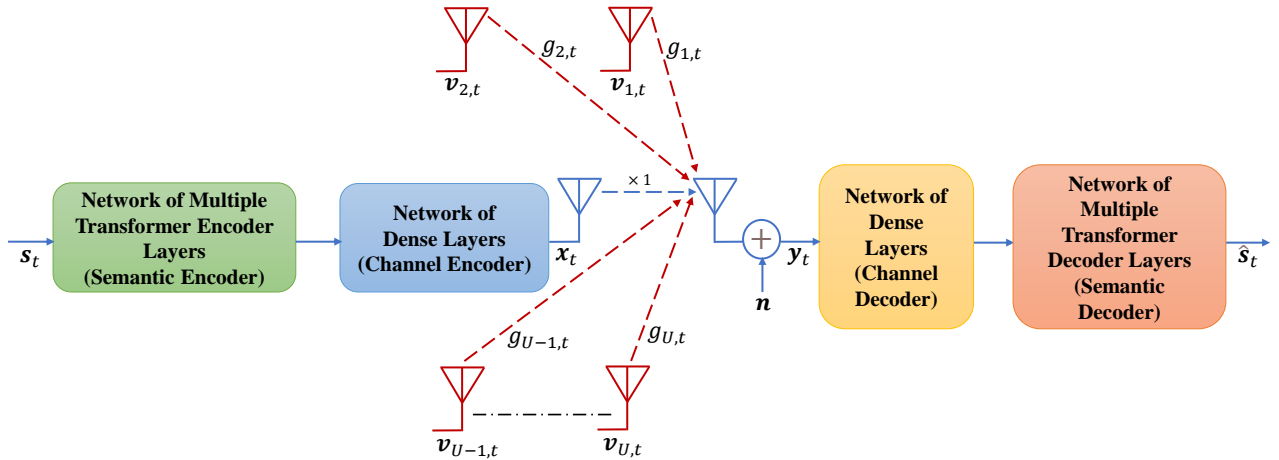


Fig. 1. System setup: During training of DeepSC, the t -th DeepSC symbol x_t is transmitted over an additive white Gaussian noise (AWGN) channel; during the testing of DeepSC, the DeepSC symbols – transmitted over an AWGN channel – are received along with the symbols of time-varying MI RFI from U ($U \geq 2$) Gaussian RFI emitters whose interference signals are received over Rayleigh fading channels.

paper documents our extensive computer experiments on the training of DeepSC and the testing of its trained models with and without MI RFI. Employing a standard SMT and NMT dataset named the proceedings of the European Parliament (*Europarl*) [29] in its training and testing, this empirical work delivers the following contributions:

- We present a step-by-step description of DeepSC’s training using Keras 2.9 with TensorFlow 2.9 as a backend.
- We perform testing of trained DeepSC models with and without MI RFI received over Rayleigh fading channels.
- We empirically demonstrate that DeepSC tends to produce semantically irrelevant sentences as the number of Gaussian RFI interferers becomes very large. This verifies our recently developed theory on the performance limits of DeepSC under interference.
- Through its detailed step-by-step procedures and implementations, this paper establishes a data preprocessing and neural processing standard for DeepSC and DeepSC-inspired text SemCom techniques.

Informed by multidisciplinary theoretical and empirical research on DL, NLP, NMT, and SemCom, this paper documents extensive details on the entire step-by-step procedures regarding the training of DeepSC followed by its testing with and without interference. This closes the existing knowledge gap – from an implementation viewpoint – that can hamper the development of many text SemCom techniques.

The remainder of this paper is organized as follows. Sec. II presents our training setup and assumptions. Sec. III details data standardization, tokenization, and vectorization. Sec. IV documents the end-to-end training of DeepSC. Sec. V reports on the testing of our trained DeepSC models with and without MI RFI. Finally, Sec. VI outlines the concluding summary and research outlook of this paper.

Notation: Scalars, vectors, and matrices (also tensors) are represented by italic letters, bold lowercase letters, and bold

uppercase letters, respectively. $:=$, \sim , $(\cdot)^T$ stand for equal by definition, distributed as, and transpose, respectively. $\mathbb{P}(\cdot)$, $\|\cdot\|$, and $\mathbb{I}\{\cdot\}$ denote probability, Euclidean norm, and an indicator function that returns one when the argument is true and 0 otherwise, respectively. $\mathbf{0}$ denotes a zero vector, \mathbf{I}_n represents an $n \times n$ identity matrix, and $[n] := \{1, 2, \dots, n\}$. \mathbb{N} , \mathbb{R} , \mathbb{R}^n , and $\mathbb{R}^{m \times n}$ denote the set of natural numbers, the set of real numbers, the set of n -dimensional vectors of real numbers, and the set of $m \times n$ real matrices, respectively. $\mathbb{R}^{m \times n \times p}$ stands for the set of $m \times n \times p$ real three-way tensors. For a row vector $\mathbf{a} \in \mathbb{R}^{1 \times n}$ and a column vector $\mathbf{b} \in \mathbb{R}^n$, the i -th element is denoted by $(\mathbf{a})_i$ and $(\mathbf{b})_i$, respectively. The dot product between two conformable vectors \mathbf{a} and \mathbf{b} is denoted as $\mathbf{a} \cdot \mathbf{b}$. $\mathcal{N}(0, \sigma^2)$ denotes a Gaussian distribution with zero mean and variance σ^2 . A random vector $\mathbf{x} := [(\mathbf{x})_1, (\mathbf{x})_2, \dots, (\mathbf{x})_n] \in \mathbb{R}^n$ is characterized statistically as $\mathbf{x} \sim \mathcal{N}(\mathbf{0}, \sigma^2 \mathbf{I}_n)$ if and only if (iff) all its elements are jointly independent and Gaussian, i.e., $(\mathbf{x})_i \sim \mathcal{N}(0, \sigma^2)$ for all $i \in [n]$.

II. TRAINING SETUP AND ASSUMPTIONS

Our theoretical work in [1] quantified the performance of a text SemCom system dubbed DeepSC suffering from radio frequency interference (RFI) that is emitted by one or more single-antenna RFI emitters. To validate our performance quantification, we carry out extensive end-to-end training of DeepSC – as shown in Fig. 2 – followed by testing without and with MI RFI. For this training and testing, we hereunder outline the experimental setup and assumptions of our extensive computer experiments, as also depicted in Fig. 1.

Let $\mathbf{s}_t := [w_{1,t}, w_{2,t}, \dots, w_{L,t}]$ be a sentence of L words to be transmitted using DeepSC during the t -th time slot.²

²Without loss of generality, we assume – throughout this work – a time-slotted system. According to (1), hence, one time slot is as long as KL times the duration of one semantic symbol.

The DeepSC transmitter first feeds s_t to a semantic encoder whose output is then fed to a channel encoder. As a result, there follows the t -th DeepSC symbol x_t that is given by [15]

$$\mathbf{x}_t := C_\alpha(S_\beta(\mathbf{s}_t)) \in \mathbb{R}^{1 \times KL}, \quad (1)$$

where $S_\beta(\cdot)$ denotes the semantic encoder network with a parameter set β , $C_\alpha(\cdot)$ represents the channel encoder network with a parameter set α , K stands for the average number of semantic symbols per word in s_t , and \mathbf{x}_t^T belongs to a set of KL -dimensional vectors of real numbers (i.e., $\mathbf{x}_t^T \in \mathbb{R}^{KL}$) because we presume – without loss of generality – real inputs. As defined in (1), the t -th DeepSC symbol then goes through an additive white Gaussian noise (AWGN) channel – which we assume without loss of generality – that yields the t -th received DeepSC signal \mathbf{y}_t equated as

$$\mathbf{y}_t := \mathbf{x}_t + \mathbf{n} \in \mathbb{R}^{1 \times KL}, \quad (2)$$

where \mathbf{n} is the contaminating AWGN which is characterized statistically as $\mathbf{n} \sim \mathcal{N}(\mathbf{0}, \sigma^2 \mathbf{I}_{KL})$. As defined in (2), the t -th received DeepSC signal \mathbf{y}_t goes through the channel decoder $C_\delta(\cdot)$ whose outputs are fed to the semantic decoder $S_\theta(\cdot)$ to produce the t -th recovered training sentence \hat{s}_t given by [15]

$$\hat{s}_t := S_\theta(C_\delta(\mathbf{y}_t)), \quad (3)$$

where the channel decoder $C_\delta(\cdot)$ and the semantic decoder $S_\theta(\cdot)$ have a parameter set δ and θ , respectively.

An end-to-end training of this text SemCom system amounts to determining – via extensive training of the DeepSC architecture shown in Fig. 2 – the (nearly) optimum semantic encoder $S_\beta(\cdot)$, channel encoder $C_\alpha(\cdot)$, channel decoder $C_\delta(\cdot)$, and semantic decoder $S_\theta(\cdot)$ that minimize the *semantic discrepancy* (semantic difference) between the t -th recovered sentence \hat{s}_t and the t -th transmitted sentence s_t for all $t \in \mathbb{N}$. Such a DL network training takes s_t as the t -th input to the end-to-end DeepSC architecture whose recovered sentence \hat{s}_t is compared with respect to (w.r.t.) a label s_t so that an end-to-end training of DeepSC resumes using the back-propagation algorithm (BackProp). This BackProp-based supervised learning problem on an end-to-end learning of DeepSC cannot, however, be formulated as a regression AI/ML problem. This is for the fact that neither computers nor deep networks can understand strings/sentences, but numbers.³

To overcome the mentioned understanding problem, one can convert each word – of a sentence – into integers (i.e., *tokenize*) and then *vectorize* each sentence into a sequence of integers, which are fed to the DeepSC network. The DeepSC network can, thus, be trained using *categorical cross-entropy* to solve a multi-level classification AI/ML problem by learning the probability of each word in a sentence while taking into account the dictionary size (vocabulary size) of a given dataset. The probability of each word in a sentence can be learned – with some accuracy – via a DeepSC training w.r.t. training labels that are the *one-hot encoded* [30] versions of the tokenized words of the t -th sentence s_t for all $t \in \mathbb{N}$.

³If computers and deep networks were able to understand strings/sentences, they would be the training inputs and the training labels of a regression AI/ML problem on NMT and text SemCom.

This leads to the implementation of our data standardization, tokenization, and vectorization, as documented below.

III. DATA STANDARDIZATION, TOKENIZATION, AND VECTORIZATION

The Europarl parallel corpora are extracted from the European Parliament’s proceedings and include versions in 21 European languages [29]. Europarl [29] is a standard dataset that has been deployed for SMT and NMT [31]. Since recently, Europarl has also been employed for the training and testing of DL-based text SemCom systems.⁴ Accordingly, we also adopt Europarl in our training and testing of DeepSC, and standardize it as follows. From Europarl’s 20 parallel corpora in [29], we first downloaded the German-English parallel corpus (193 MB) that comprises 1,920,209 (≈ 2 million) sentences and 47,818,827 (≈ 48 million) English words. We then *unzipped* the downloaded parallel corpus and uploaded the English corpus (named “europarl-v7.de-en.en”) into our working directories located at graphics processing unit (GPU) clusters of the Digital Research Alliance of Canada [32] named *Béluga* [33] and *Graham* [34].

Our uploaded English corpus needs to be standardized (or *cleaned*) since all non-printable characters, punctuation characters, and words that comprise non-alphabetic characters have to be removed [31], [35]. This necessitates the implementation of data standardization, which is highlighted below.

A. Data Standardization

We begin our data standardization (or *data cleaning*) by uploading the Europarl text into memory. To this end, on our working directory in both *Béluga* and *Graham*, we first load the Europarl English document into memory by opening it as a read only file, reading all its text, closing the file, and then returning it as a blob of text. We then split the loaded text into sentences by splitting it on new line characters. We then clean each of these sentences by normalizing it to unicode characters, tokenizing it on white space, converting it to lowercase, removing punctuation and non-printable characters from each of its tokens, removing its tokens with numbers in them, and finally storing it as a string. We then return a list of clean sentences and save it to a file, which we henceforward refer to as our saved Europarl document of clean sentences.

Our saved Europarl document of clean sentences can comprise many less frequent words – which hardly help DeepSC to learn a text SemCom system efficiently – that only increase the vocabulary size to the extent that an *out of memory error* (OOM error) is triggered by *Béluga* and *Graham*. This justifies the need for our implementation of vocabulary reduction (or dictionary size reduction), as described below.

B. Data Vocabulary Reduction

Our implementation of a vocabulary reduction reduces the vocabulary of our saved Europarl document of clean sentences and marks all *out of vocabulary* (OOV) words with a special

⁴Europarl is a popular dataset in the design of many text SemCom systems (see [16, Sec. III]) such as DeepSC.

NMT token named “unk”. To this end, we first load our saved Europarl document of clean sentences. From these loaded clean sentences, we create a vocabulary. From this vocabulary, we remove all words that have an occurrence below a minimum specified threshold and generate our trimmed vocabulary. By taking our trimmed vocabulary and the loaded clean sentences as inputs, we create our Europarl document of clean sentences with reduced vocabulary by removing all words that are not in our trimmed vocabulary and marking their removal with “unk” – similar to the work in [31]. We then save our created Europarl document of clean sentences with reduced vocabulary, which we will employ in the preparation of our training, validation, and testing sets.

By trimming words that appear less than 20 times in our saved Europarl document of clean sentences, we were able to reduce the vocabulary size from 102,917 to 22,897. In other words, our saved Europarl document of clean sentences with reduced vocabulary has a vocabulary size (dictionary size) of 22,897 words. By loading this saved Europarl document that consists of 1,920,209 sentences, we saved the first 1,900,000 sentences as the overall dataset sentences. From these overall dataset sentences, we saved the first 100,000, the next 1,500,000, and the last 300,000 sentences as testing sentences, training sentences, and validation sentences, respectively. Deploying the saved testing sentences, training sentences, and validation sentences, we prepared our testing sets, training sets, and validation sets, respectively, as documented below.

C. Preparation of the Testing, Training, and Validation Sets

In the preparation of our testing, training, and validation sets, *data tokenization* and *data vectorization* were needed, as highlighted below.

1) *Data Tokenization*: As neither DL networks nor DeepSC take strings as input, each word of the overall dataset sentences must be encoded into numbers and all its comprising sentences must be converted (or mapped) to sequences of numbers. This is exactly what is termed data tokenization (or text tokenization) in NMT. In our text tokenization, which is needed in the preparation of our testing, training, and validation sets, we exploited the Keras *Tokenizer* class [36] to map words to integers and fed the overall dataset sentences (1.9 million) to a Keras function named `fit_on_texts()` [36]. This returned tokenizer was then fed to the data vectorizer for data vectorization (or data encoding).

2) *Data Vectorization*: Every input and output sequence – of the testing, training, and validation sets – should be encoded to integers and padded/truncated to the optimal⁵ length L , which is also the number of input neurons of a DL network, such as DeepSC, that will not trigger an OOM error. This is exactly what data vectorization (or data encoding) is and we have accomplished this using an encoding function that takes the tokenizer of Sec. III-C1, length $L = 30$, and the

⁵A number of NMT works, such as the work in [35], encoded (to integers) and padded each input sequence to the length of the longest sequence in a list of sentences. Such a strategy has triggered an OOM error in both Béluga and Graham. In our DeepSC training, we found $L = 30$ to be an optimal length that does not cause an OOM error. Hence, we truncated and zero padded sequences that have a length of greater than and less than 30, respectively.

testing sentences, training sentences, or validation sentences. Specifically, this encoding function executes the following on the testing, training, and validation sentences:

- It transforms each sentence of the testing sentences, training sentences, and validation sentences (whatever is fed to it) to a sequence of integers by employing the tokenizer of Sec. III-C1 and the Keras function `texts_to_sequences()` [36].
- It then *vectorizes* each sequence of integers to an integer sequence of (the same) length $L = 30$ by post padding with zeros or truncating using the Keras function `tf.keras.utils.pad_sequences()` [37].

Each token of the produced sequences (of equal length $L = 30$) needs to be labeled, as highlighted below.

3) *Data Labeling*: Since the DeepSC model is trained to learn the probability of each word (via its assigned unique token) w.r.t. its `softmax` prediction layer, each token of a data vectorized sequence has to be *one-hot encoded*. To accomplish this, we exploit the Keras function `tf.keras.utils.to_categorical()` [38] and apply it to each data vectorized sequence of Sec. III-C2. This one-hot encoding is also fed the number of possible classes that is equal to the vocabulary size (dictionary size) of our tokenizer per Sec. III-C1. The vocabulary size of our tokenizer is equal to the number of unique word indices in our Sec. III-C1’s tokenizer plus one,⁶ which is also the number of output neurons in the `softmax` prediction layer of the DeepSC architecture shown in Fig. 2.

According to the data tokenization, data vectorization, and data labeling of Secs. III-C1, III-C2, and III-C3, we prepare our training, validation, and testing sets. When it comes to our testing set, we do not need testing labels because we assess – without and with RFI – the performance of our trained DeepSC model using a SemCom performance assessment metric named *sentence similarity* [39]. Hence, we only prepare the testing inputs by first loading the saved 100,000 testing sentences (from Sec. III-B) that we tokenized and vectorized per Secs. III-C1 and III-C2, respectively. This results in testing inputs of $100,000 \times 30$ (non-negative) integers. To continue to the preparation of our training set, we prepare our training set by implementing the following four steps in Keras with TensorFlow as a backend:

- We first load our saved 1.5 million training sentences (from Sec. III-B) to our working directories in Béluga and Graham.
- We then tokenize and vectorize – per Secs. III-C1 and III-C2, respectively – each training sentence to produce our training inputs of $1,500,000 \times 30$ (non-negative) integers.
- We then feed the produced training inputs to a Keras generator function – implemented using `tf.keras.utils.Sequence` [40] along with the data labeling per Sec. III-C3 – that also takes a batch size $B = 50$ and a vocabulary size of 22,899.

⁶In our DeepSC training and testing, accordingly, the vocabulary size was equal to 22,899. Note that this dictionary size was calculated after vocabulary reduction per Sec. III-B.

- Our coded Keras generator function⁷ then returns our training inputs of 50×30 (non-negative) integers and training labels of $50 \times 30 \times 22,899$ binary integers (zeros or ones) for every training batch.

Similarly, we prepare our validation set by executing the following four steps in Keras with TensorFlow as a backend:

- We first load our saved 300,000 validation sentences (from Sec. III-B) to our working directories in Béluga and Graham.
- We then tokenize and vectorize each validation sentence – per Secs. III-C1 and III-C2, respectively – to yield our validation inputs of $300,000 \times 30$ (non-negative) integers.
- We then feed the validation inputs to the aforementioned Keras generator function that also takes a batch size of 50 and a vocabulary size of 22,899 amongst its inputs.
- Our coded Keras generator function then returns our validation inputs of 50×30 (non-negative) integers and validation labels of $50 \times 30 \times 22,899$ binary integers for every validation batch.

Our prepared training and validation sets – already returned by our Keras generator – are then fed to the Keras `model.fit_generator()` [41] training function after defining and compiling the DeepSC model, as detailed below.

IV. END-TO-END TRAINING OF DEEPC

In this section, we detail our end-to-end training of DeepSC. Specifically, we present the end-to-end training architecture of DeepSC, the DeepSC model definition, and the training results of DeepSC that we obtained using Adam [42], as an optimizer. We now begin with DeepSC’s end-to-end training architecture.

A. The End-to-End Training Architecture of DeepSC

The DeepSC architecture (with real inputs) that we employ in our end-to-end training of DeepSC is depicted in Fig. 2.⁸ As can be seen in Fig. 2, which depicts the forward-propagation during *one batch* of training inputs with a batch size B , a matrix $\mathbf{S} \in \mathbb{R}^{B \times L}$ of training inputs is fed to an embedding layer. The embedding layer of Fig. 2 then turns (positive-integer) indexes into dense vectors of fixed size [44] and yields an embedding tensor $\mathbf{E} \in \mathbb{R}^{B \times L \times E}$. The embedding tensor \mathbf{E} is then fed to the semantic encoder made of three cascaded Transformer encoders – per Fig. 3 – that produce rich representations (for every embedded word vector) which constitute an output tensor $\mathbf{M} \in \mathbb{R}^{B \times L \times E}$. Being a tensor of

⁷Note that our coded Keras generator function randomly shuffled our training and validation sets – between epochs – on every epoch end. Note also that we implemented the data labeling of Sec. III-C3 inside our coded Keras generator function in order to overcome an OOM error, which we came across in both Béluga and Graham.

⁸In their published work [15], the DeepSC authors first trained the *MINE* (mutual information neural estimation) network from [43] to maximize the mutual information $I(\mathbf{x}_t; \mathbf{y}_t)$. They then used the loss of this trained MINE network to tweak the loss of the DeepSC architecture – shown in Fig. 2 – during its training. The authors state that this would maximize the achieved data rate during the DeepSC transceiver training [15]. However, since our problem is all about assessing the impact of interference/RFI to *sentence similarity* between the transmitted and recovered sentences of an already trained DeepSC, we discarded to train the MINE network and directly trained the DeepSC architecture schematized in Fig. 2.

semantically-encoded symbols, the output tensor \mathbf{M} is then fed to a channel encoder⁹ made of two cascaded Dense layers [45] that give an output tensor $\mathbf{X} \in \mathbb{R}^{B \times L \times K}$. The channel-encoded semantic symbols are then reshaped – to produce $\mathbf{X} \in \mathbb{R}^{B \times K \times L}$ – and transmitted through an AWGN channel modeled by a linear Dense layer.

The AWGN channel contaminates its input $\mathbf{X} \in \mathbb{R}^{B \times K \times L}$ and produces an output that is reshaped into a three-way tensor $\mathbf{Y} \in \mathbb{R}^{B \times L \times K}$. The tensor \mathbf{Y} is then inputted to a channel decoder that is composed of two cascaded Dense layers that yield a tensor $\hat{\mathbf{M}} \in \mathbb{R}^{B \times L \times E}$, which is a tensor of recovered semantically-encoded symbols. The tensor $\hat{\mathbf{M}} \in \mathbb{R}^{B \times L \times E}$ is then fed to a semantic decoder that is composed of three cascaded Transformer decoders – with no cross-attention as in Fig. 3 – whose outputs are fed to a softmax prediction layer to produce a matrix $\hat{\mathbf{S}} \in \mathbb{R}^{B \times L}$, which is a matrix of recovered sentences.

Consistent with Figs. 2 and 3, we now continue with the DeepSC model definition.

B. Model Definition of DeepSC

Without loss of generality and out of care for not causing an OOM error in both Béluga and Graham, we defined two DeepSC models for our training. These models are a narrow model named *narrow DeepSC* and a relatively wide model named *relatively wide DeepSC*. These models are parameterized by (K, H, V, E, L) , where (K, E, L) are the DeepSC parameters defined in the caption of Fig. 2, H is the number of heads of a Transformer encoder/decoder, and V is the hidden layer dimension of the Transformer encoder’s/decoder’s feedforward network per Fig. 3.

Narrow DeepSC is parameterized by $(K, H, V, E, L) = (8, 10, 32, 32, 30)$. The narrow DeepSC model, along with its layer parameters and connections, are schematized in Figs. 12 and 13 (see Appendix A), respectively. Relatively wide DeepSC is parameterized by $(K, H, V, E, L) = (8, 10, 32, 64, 30)$. The relatively wide DeepSC model, along with its layer parameters and connections, are diagrammed in Figs. 14 and 15 (see Appendix A), respectively. In what follows, we explain how we define and generate the relatively wide DeepSC model of Figs. 14 and 15 (see Appendix A) and the narrow DeepSC model of Figs. 12 and 13 (see Appendix A) using Keras with TensorFlow as a backend.

We employ the Keras model class [47] – `tf.keras.Model()` – to define our two DeepSC models. These models are returned by our DeepSC function – implemented in Keras with TensorFlow as a backend – that takes the target vocabulary size (or dictionary size), K , H , V , E , and L as its inputs. In this function, we first specify the DeepSC model – that is being defined – input and its shape using the Keras function `tf.keras.Input()` [47]. This input layer is then fed to an embedding layer, implemented using the

⁹Note that both the channel encoder and channel decoder can be composed of numerous cascaded Dense layers, which are deep networks in their own right. Nonetheless, such deeper and (possibly) *overfitted architectures* led to – as witnessed in our computer experiments – *gradient explosion* and/or *gradient vanishing*.

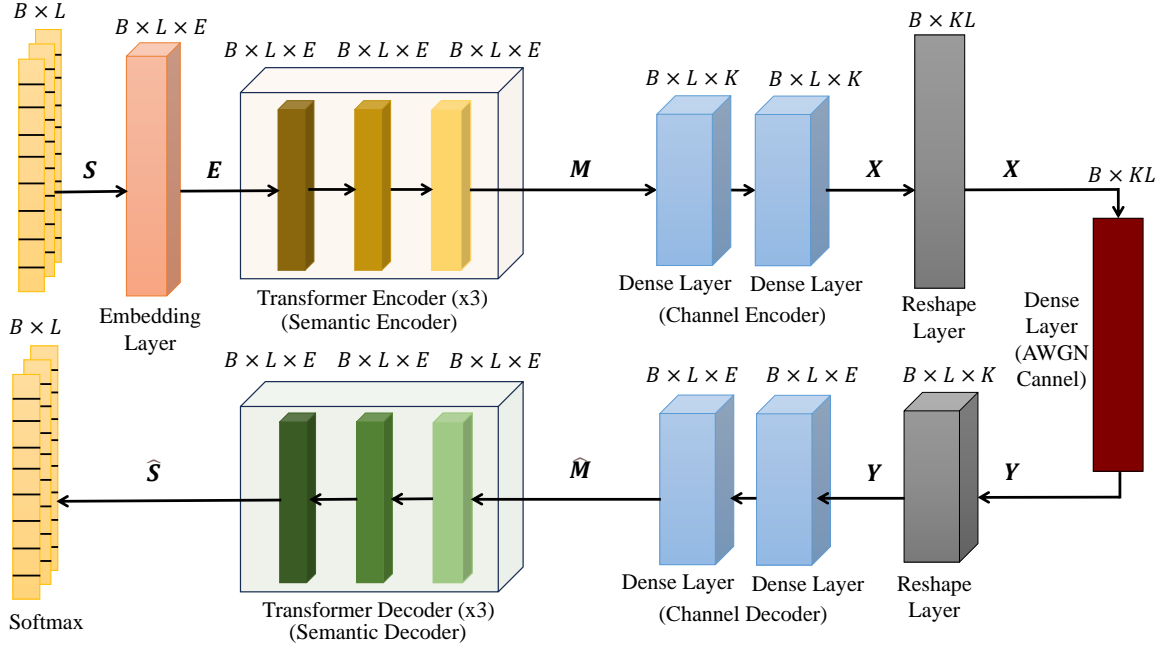


Fig. 2. The DeepSC architecture (with real inputs) under our training and testing. (Hyper)parameters: B – batch size; L – number of words per a transmitted sentence (i.e., a transmitted sentence length); E – embedding dimension (the output dimension of an embedding layer); K – average number of semantic symbols per word in a given transmitted sentence.

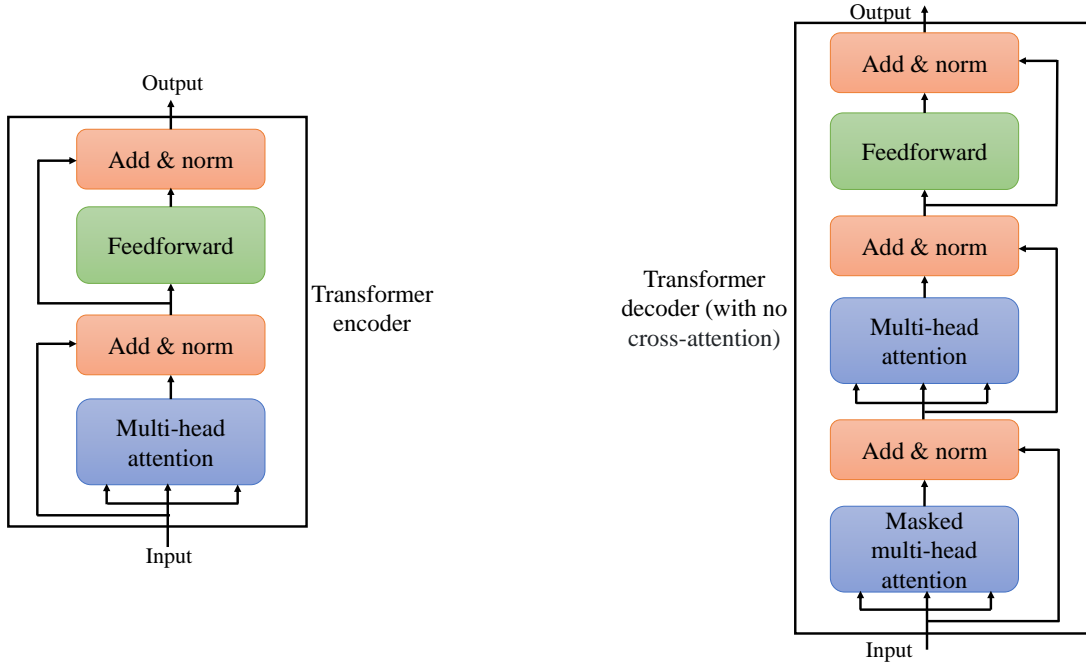


Fig. 3. Transformer encoder and Transformer decoder (with no cross-attention) [46].

Keras function `tf.keras.layers.Embedding()` [44], with an input dimension L and an output dimension (embedding dimension) E . The output of this embedding layer is then fed to three cascaded Transformer encoders that we implement using the Keras function `keras_nlp.layers.TransformerEncoder()` [48]. The three Transformer encoders are implemented to have V and H as the hidden size of their feedforward network

and the number of heads in their corresponding multi-head attention layer, respectively, linear activation function, and the `he_normal` initializer [49] as their respective kernel initializer.

The output of the three cascaded Transformer encoders are then fed to two cascaded Dense layers, realized using the Keras function `tf.keras.layers.Dense()` [45]. The two Dense layers have a ReLU activation function

and the `he_normal` initializer [49] as their kernel initializer. The output tensor of these cascaded Dense layers is reshaped into a matrix using the Keras reshape layer `tf.keras.layers.Reshape()` [53] and fed to the non-trainable (linear) Dense layer that models our presumed AWGN channel. As noted in [54], we initialize this linear AWGN layer with the `Identity()` initializer [49] and `tf.keras.initializers.RandomNormal()` initializer [49] (with zero mean and variance 0.1) as its kernel initializer and bias initializer, respectively. The AWGN channel output is then reshaped – using the Keras reshape layer `tf.keras.layers.Reshape()` [53] – and fed to two other cascaded Dense layers realized using the Keras function `tf.keras.layers.Dense()` [45]. These Dense layers also have a ReLU activation function and the `he_normal` initializer [49] as their kernel initializer, realizing the channel decoder.

The channel decoder’s output is then inputted to three cascaded Transformer decoders implemented using the function `keras_nlp.layers.TransformerDecoder()` [55] which is set to have no cross-attention. The three Transformer decoders are also implemented to have V and H as the hidden size of their feedforward network and the number of heads in their multi-head attention layer, respectively, linear activation function, and the `he_normal` initializer [49] as their corresponding kernel initializer. These cascaded Transformer decoders constitute a semantic decoder whose output is fed to a softmax prediction layer realized using the function `tf.keras.layers.Dense()` [45], with its

output dimension equal to the target vocabulary size.

Produced by cascading the above-detailed Keras functions, we finally generated narrow DeepSC using $(K, H, V, E, L) = (8, 10, 32, 32, 30)$ and relatively wide DeepSC using $(K, H, V, E, L) = (8, 10, 32, 64, 30)$. These models are *compiled* using the Adam [42] optimizer, `categorical_crossentropy` loss, and accuracy as a classification metric. This model compiling make us ready to start our DeepSC training, as detailed below.

C. Training Results of DeepSC

Employing the generated narrow DeepSC and relatively wide DeepSC models, we carry out extensive computer experiments on their training using the Adam optimizer¹⁰ [42] and the (hyper)parameters in Table I such as the four *Keras callbacks* [52]. Specifically, we deploy the Keras `model.fit_generator()` [41] function that is fed with the training and validation sets (generated per Secs. III-C1, III-C2, and III-C3), maximum epochs and steps per epoch, validation steps, and Keras callbacks to extensively train both the narrow DeepSC and relatively wide DeepSC models.

Our final training is conducted in Graham using 4 GPUs simultaneously, in line with a distributed training strategy called with `tf.distribute.MirroredStrategy()`.

¹⁰We have also performed extensive DeepSC training using SGD with momentum [50] and RMSprop [51]. Although we have obtained much better training results with SGD with Momentum than with RMSprop, none of these optimizers has led to better training results than the ones we have obtained with Adam.

TABLE I
DEEPC TRAINING (HYPER)PARAMETERS UNLESS OTHERWISE MENTIONED.

(Hyper)parameters	Type/Value	Remark(s)
Learning rate	0.0002	This initial learning rate has led to our best DeepSC training performance.
Epoch size	100	Maximum epoch size.
Batch size	50	We tried both large and small batch sizes. The latter yielded a better training performance (though it comes at a price of slow convergence).
Optimizer	Adam [42]	We experimented with SGD with momentum [50], RMSprop [51], and Adam [42]. Adam led to our best training result.
Activation function (for Dense layers)	ReLU	All Dense layers are equipped with ReLU activation function except our linear Dense layer that models the AWGN channel and our softmax prediction layer, which is the last layer of DeepSC.
Layer weight initializer (for most layers)	<code>he_normal</code> [49]	Transformer encoder layers, Transformer decoder layers, and all Dense layers are initialized with <code>he_normal</code> except the linear Dense layer that modeled our presumed AWGN channel. This layer was initialized with the Keras <code>Identity()</code> [49] initializer.
Bias initializer (for most layers)	None	No bias initializer is used on all DeepSC layers except on the linear Dense layer – that models our assumed AWGN channel – which is initialized by the Keras <code>RandomNormal()</code> initializer [49].
σ	0.1	$\sigma^2 = 0.01$ W is the considered noise power during our training/testing.
Narrow DeepSC	$(K, H, V, E, L) = (8, 10, 32, 32, 30)$	The narrow DeepSC model, along with its layer parameters and connections, are schematized in Figs. 12 and 13.
Relatively wide DeepSC	$(K, H, V, E, L) = (8, 10, 32, 64, 30)$	The relatively wide DeepSC model, along with its layer parameters and connections, are diagrammed in Figs. 14 and 15.
Training set size	1.5 million	The training set is prepared per the data tokenization, data vectorization, and data labeling of Secs. III-C1, III-C2, and III-C3.
Validation set size	300,000	The validation set is prepared per the data tokenization, data vectorization, and data labeling of Secs. III-C1, III-C2, and III-C3.
Keras <i>callbacks</i> [52]	Four callbacks	We use <i>Model checkpointing</i> , <i>TensorBoard</i> , <i>learning rate reduction</i> , and <i>early stopping</i> callbacks [52, Ch. 7]. Early stopping and learning rate reduction are set to have patience over 10 and 5 epochs, respectively. Per every five epochs that lead to a training stagnation w.r.t. the monitored validation losses, the learning rate reduction Keras callback is set to reduce the learning rate by 0.1.

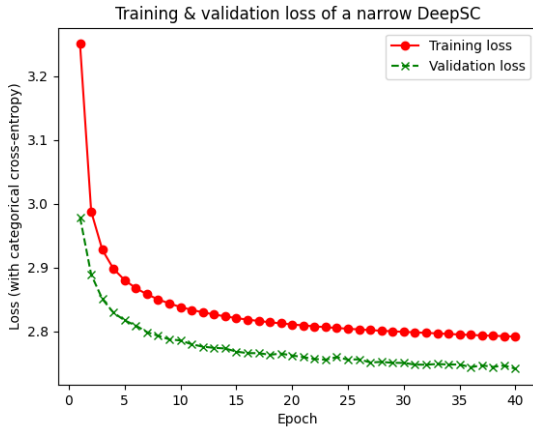


Fig. 4. Training and validation loss of narrow DeepSC when the considered maximum epoch size is 40.

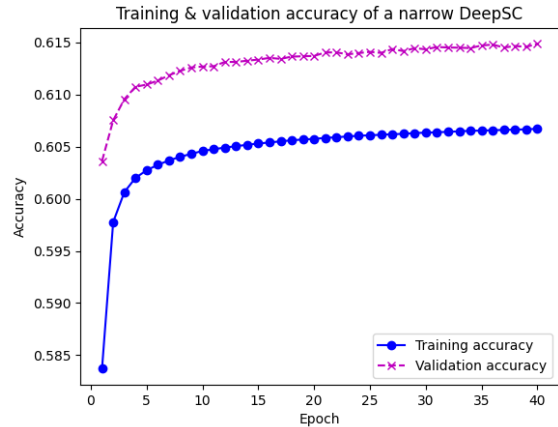


Fig. 5. Training and validation accuracy of narrow DeepSC when the considered maximum epoch size is 40.

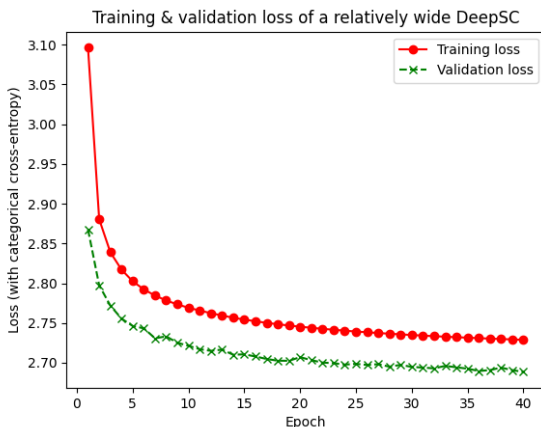


Fig. 6. Training and validation loss of relatively wide DeepSC when the considered maximum epoch size is 40.

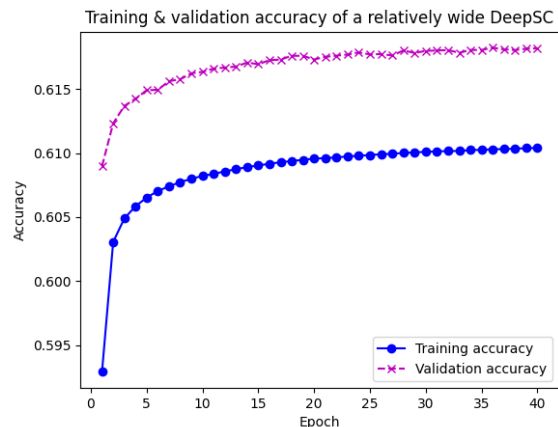


Fig. 7. Training and validation accuracy of relatively wide DeepSC when the considered maximum epoch size is 40.

Specifically, we deploy Graham’s four NVIDIA T4 Turing GPUs (16GB memory) [34] in parallel to train both the narrow DeepSC model (see Fig. 12) and the relatively wide DeepSC model (see Fig. 14) for about four days. This extensive training and optimization lead to the following training results for narrow DeepSC and relatively wide DeepSC, as reported in Secs. IV-C1 and IV-C2, respectively.

1) *Training Results of Narrow DeepSC*: Figs. 4 and 5 show the training and validation loss and the training and validation accuracy of the narrow DeepSC model, respectively. These results are the best results – among many training results – that we have achieved for narrow DeepSC with the (hyper)parameters in Table I, especially, with 1.5 million and 300, 000 training and validation sentences, respectively. As it can be seen in Fig. 4, the training and validation loss of narrow DeepSC doesn’t meaningfully decrease after 20 epochs, where there is a very small improvement for every epoch that is greater than 20.

From Fig. 5, it is observed that the training and validation accuracy of narrow DeepSC consistently improves until the end of the 40-th epoch, especially the validation accuracy. By the 40-th epoch, narrow DeepSC attains a training and

validation accuracy slightly higher than 60.5% and nearly 61.5%, respectively. Although 61.5% is hardly a high validation accuracy, the result is considerable for a DL-based multi-class classification problem with 22,899 classes (of words), which correspond to the dictionary size per Appendix A.

2) *Training Results of Relatively Wide DeepSC*: Figs. 6 and 7 depict the training and validation loss and the training and validation accuracy of the relatively wide DeepSC model, respectively. These results are the best results we have obtained – among the many training results we obtained – for relatively wide DeepSC with the (hyper)parameters in Table I, especially, with 1.5 million and 300, 000 training and validation sentences, respectively. As shown in Fig. 6, relatively DeepSC manifests a training stagnation after the 25-th epoch w.r.t. its training and validation loss though there is a minute of improvement for every epoch that is greater than 25.

From Fig. 7, it is observed that the training and validation accuracy of relatively wide DeepSC also steadily improves until the 40-th epoch, especially the validation accuracy. By the end of the 40-th epoch, relatively wide DeepSC achieves a training and validation accuracy of nearly 61% and 62%, respectively. These validation accuracy percentages demon-

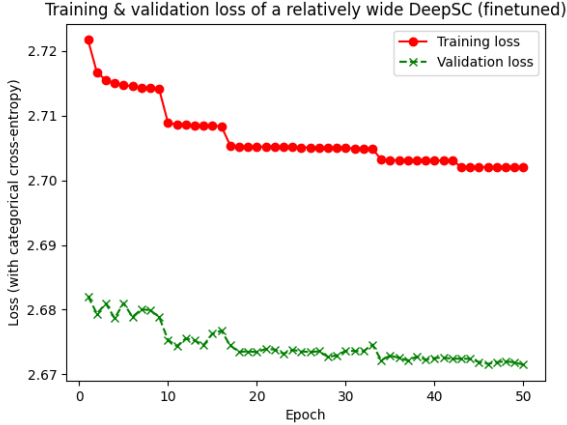


Fig. 8. Training and validation loss of relatively wide trained and finetuned DeepSC when the considered initial learning rate and maximum epoch size are 0.0001 and 50, respectively.

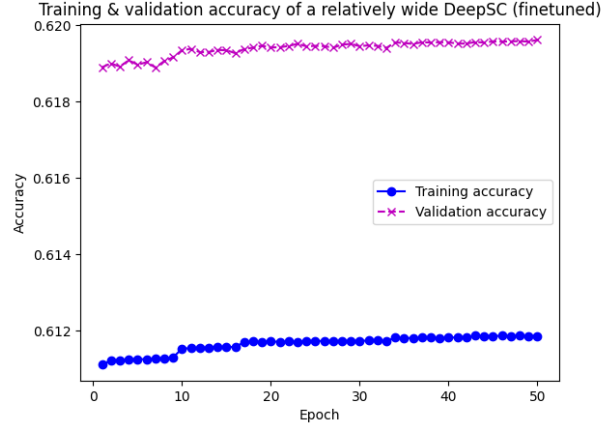


Fig. 9. Training and validation accuracy of relatively wide trained and finetuned DeepSC when the considered initial learning rate and maximum epoch size are 0.0001 and 50, respectively.

strate an improvement compared to the training performance of narrow DeepSC and are crucial results for a DL-based multi-class classification problem with 22,899 classes (of words). Meanwhile, in the hope of producing trained DeepSC models that achieve better classification accuracy, we also train both narrow DeepSC and relatively wide DeepSC models for seven days using Graham’s four NVIDIA T4 Turing (16GB memory) GPUs [34] in parallel while employing the parameters in Table I. These narrow DeepSC and relatively wide DeepSC trained models slightly improve narrow DeepSC’s and relatively wide DeepSC’s training/validation performance shown in Figs. 4-5 and Figs. 6-7, respectively. Similar to the trend observed in these plots, the seven-day-trained relatively wide DeepSC model produces better training and validation accuracy than the seven-day-trained narrow DeepSC. We name this relatively wide DeepSC model “DeepSC-Training-0814-I1” which we finetune, as detailed below.

3) *Training Results of Relatively Wide Trained and Finetuned DeepSC*: After setting all layers, apart from the AWGN channel layer, of the trained relatively wide DeepSC model named “DeepSC-Training-0814-I1” to trainable mode, we finetune “DeepSC-Training-0814-I1” for nearly five days using Graham’s four NVIDIA T4 Turing (16GB memory) GPUs [34] in parallel. This led to Figs. 8 and 9 that depict the training and validation loss of the relatively wide trained and finetuned DeepSC and the training and validation accuracy of relatively wide trained and finetuned DeepSC, respectively. Concerning the former, Fig. 8 shows that the relatively wide trained and finetuned DeepSC delivers a 0.02 and 0.01 improvement in the training and validation loss, respectively, at the end of the 50-th epoch (after nearly five days of training). By the same token, Fig. 9 demonstrates that the relatively wide trained and finetuned DeepSC produces nearly a 0.01 improvement in training and validation accuracy, after nearly five days of training.

Meanwhile, we name our relatively wide trained and finetuned DeepSC model “DeepSC-Training-0822-I1” which we also employ in our testing along with our already trained relatively wide DeepSC model named “DeepSC-Training-0814-I1”, as documented below.

V. TESTING OF THE TRAINED DEEPS SC MODELS WITH(OUT) MULTI-INTERFERER RFI

In this section, the testing setup and assumptions, the testing procedures, and the testing results of the above trained DeepSC models with and without MI RFI are detailed. We start with our testing setup and assumptions.

A. Testing Setup and Assumptions

The testing of our trained relatively wide DeepSC models, i.e., “DeepSC-Training-0814-I1” and “DeepSC-Training-0822-I1”, considers the cases where no RFI and MI RFI (from U RFI emitters) is received by the DeepSC receiver. For these models, their respective DeepSC symbols are expressed as

$$\tilde{\mathbf{x}}_t := C_{\tilde{\alpha}}(S_{\tilde{\beta}}(\tilde{\mathbf{s}}_t)) \in \mathbb{R}^{1 \times KL} \quad (4a)$$

$$\tilde{\mathbf{x}}_t^f := C_{\tilde{\alpha}}^f(S_{\tilde{\beta}}^f(\tilde{\mathbf{s}}_t)) \in \mathbb{R}^{1 \times KL}, \quad (4b)$$

where $\tilde{\mathbf{x}}_t$ and $\tilde{\mathbf{x}}_t^f$ are the DeepSC symbols of the relatively wide trained DeepSC model and the relatively wide trained and finetuned DeepSC model, respectively; $S_{\tilde{\beta}}(\cdot)$ and $C_{\tilde{\alpha}}(\cdot)$ are the relatively wide trained DeepSC model’s semantic encoder network with a parameter set $\tilde{\beta}$ and channel encoder network with a parameter set $\tilde{\alpha}$, respectively; $S_{\tilde{\beta}}^f(\cdot)$ and $C_{\tilde{\alpha}}^f(\cdot)$ are the relatively wide trained and finetuned DeepSC model’s semantic encoder network with a parameter set $\tilde{\beta}$ and channel encoder network with a parameter set $\tilde{\alpha}$, respectively; and $\tilde{\mathbf{s}}_t$ is the t -th testing sentence encoded and prepared according to Sec. III-C. For the case of no MI RFI, the received DeepSC signals during the t -th time slot are given by

$$\tilde{\mathbf{y}}_t := \tilde{\mathbf{x}}_t + \mathbf{n} \in \mathbb{R}^{1 \times KL} \quad (5a)$$

$$\tilde{\mathbf{y}}_t^f := \tilde{\mathbf{x}}_t^f + \mathbf{n} \in \mathbb{R}^{1 \times KL}, \quad (5b)$$

where $\tilde{\mathbf{y}}_t$ and $\tilde{\mathbf{y}}_t^f$ are the DeepSC signals of the relatively wide trained DeepSC model and the relatively wide trained and finetuned DeepSC model, respectively. For the MI RFI scenario, we presume – without loss of generality – that the trained channel decoders receive time-varying MI RFI from U Gaussian RFI (i.e., broadband RFI) [56]–[59] emitters

whose interference signals are received over Rayleigh fading channels. Under MI RFI, the received DeepSC signals during the t -th time slot are equated as

$$\tilde{\mathbf{y}}_t := \tilde{\mathbf{x}}_t + \sum_{u=1}^U g_{u,t} \mathbf{v}_{u,t} + \mathbf{n} \in \mathbb{R}^{1 \times KL} \quad (6a)$$

$$\tilde{\mathbf{y}}_t^f := \tilde{\mathbf{x}}_t^f + \sum_{u=1}^U g_{u,t}^f \mathbf{v}_{u,t}^f + \mathbf{n} \in \mathbb{R}^{1 \times KL}, \quad (6b)$$

where $\tilde{\mathbf{x}}_t$ and $\tilde{\mathbf{x}}_t^f$ are defined in (4a) and (4b), respectively; $g_{u,t}, g_{u,t}^f \sim \mathcal{N}(0, 1)$ are the channel coefficients¹¹ of the u -th RFI during the t -th time slot; and $(\mathbf{v}_{u,t})_i, (\mathbf{v}_{u,t}^f)_i \sim \mathcal{N}(0, 10)$ are the respective Gaussian RFI signals – with an assumed power that is equal to 10 W – of the u -th Gaussian RFI emitted during the t -th time slot for all $i \in [KL]$. As defined in (6a) and (6b), $\tilde{\mathbf{y}}_t$ and $\tilde{\mathbf{y}}_t^f$ then go through – per Fig. 2 – the trained channel decoders whose outputs are fed to the trained semantic decoders to produce the t -th recovered testing sentences $\hat{\tilde{\mathbf{s}}}_t$ and $\hat{\tilde{\mathbf{s}}}_t^f$ that can be expressed as

$$\hat{\tilde{\mathbf{s}}}_t := S_{\hat{\theta}}(C_{\hat{\delta}}(\tilde{\mathbf{y}}_t)) \quad (7a)$$

$$\hat{\tilde{\mathbf{s}}}_t^f := S_{\hat{\theta}}^f(C_{\hat{\delta}}^f(\tilde{\mathbf{y}}_t^f)), \quad (7b)$$

where $C_{\hat{\delta}}(\cdot)$ and $S_{\hat{\theta}}(\cdot)$ are the relatively wide trained DeepSC model's channel decoder network with parameter set $\hat{\delta}$ and semantic decoder network with parameter set $\hat{\theta}$, respectively; $C_{\hat{\delta}}^f(\cdot)$ and $S_{\hat{\theta}}^f(\cdot)$ are the relatively wide trained and finetuned DeepSC model's channel decoder network with parameter set $\hat{\delta}$ and semantic decoder network with parameter set $\hat{\theta}$, respectively. Now, $\{\tilde{\mathbf{s}}_t, \hat{\tilde{\mathbf{s}}}_t\}$ and $\{\tilde{\mathbf{s}}_t^f, \hat{\tilde{\mathbf{s}}}_t^f\}$ have to be compared from a semantic vantage point for all $t \in \mathbb{N}$.

Although our training was conducted using categorical cross-entropy loss while setting classification accuracy as a metric, this performance assessment metric is not a proper semantic metric for a text SemCom [39]. Consequently, we adopt our recently proposed semantic metric, named the (*upper tail*) *probability of semantic similarity* $p(\eta_{\min})$ [1], to evaluate the testing performance of the relatively wide trained DeepSC model and the relatively wide trained and finetuned DeepSC model w.r.t. a minimum semantic similarity $\eta_{\min} \in [0, 1]$. For $\eta_{\min} \in [0, 1]$, this metric is specifically defined for the t -th transmitted and recovered sentence pairs $\{\tilde{\mathbf{s}}_t, \hat{\tilde{\mathbf{s}}}_t\}$ and $\{\tilde{\mathbf{s}}_t^f, \hat{\tilde{\mathbf{s}}}_t^f\}$ as [1, eq. (9)]

$$p(\eta_{\min}) := \mathbb{P}(\eta(\tilde{\mathbf{s}}_t, \hat{\tilde{\mathbf{s}}}_t) \geq \eta_{\min}) \quad (8a)$$

$$p(\eta_{\min}) := \mathbb{P}(\eta(\tilde{\mathbf{s}}_t, \hat{\tilde{\mathbf{s}}}_t^f) \geq \eta_{\min}), \quad (8b)$$

where $\eta(\tilde{\mathbf{s}}_t, \hat{\tilde{\mathbf{s}}}_t)$ denotes the semantic similarity between $\tilde{\mathbf{s}}_t$ and $\hat{\tilde{\mathbf{s}}}_t$; $\eta(\tilde{\mathbf{s}}_t, \hat{\tilde{\mathbf{s}}}_t^f)$ stands for the semantic similarity between $\tilde{\mathbf{s}}_t$ and $\hat{\tilde{\mathbf{s}}}_t^f$; and $\eta(\cdot, \cdot)$ is the semantic similarity (or sentence similarity) function that is often estimated using large pre-trained Transformers, such as the *HuggingFace's* (see [60]) *sentence Transformers* [61]. Among these Transformers, we

¹¹During the reception of the t -th DeepSC symbol, the channel coefficients $g_{u,t}, g_{u,t}^f \sim \mathcal{N}(0, 1)$ remain constant for the duration of the t -th DeepSC symbol, which is equal to KL times the duration of each semantic symbol, signifying slowly-varying MI RFI.

deploy – for simplicity and without loss of generality – *HuggingFace's* lightweight state-of-the-art sentence Transformer dubbed `all-MiniLM-L6-v2` [62].¹²

Using our testing sentences (encoded and prepared per Sec. III-C), we numerically estimate – w.r.t. (8a) and (8b) – the probability of semantic similarity exhibited by the relatively wide trained DeepSC model and the relatively wide trained and finetuned DeepSC model as

$$p(\eta_{\min}) = \frac{1}{N} \sum_{t=1}^N \mathbb{I}\{\eta(\tilde{\mathbf{s}}_t, \hat{\tilde{\mathbf{s}}}_t) \geq \eta_{\min}\} \quad (9a)$$

$$p(\eta_{\min}) = \frac{1}{N} \sum_{t=1}^N \mathbb{I}\{\eta(\tilde{\mathbf{s}}_t, \hat{\tilde{\mathbf{s}}}_t^f) \geq \eta_{\min}\}, \quad (9b)$$

where N is the number of testing sentences employed to assess the manifested probability of semantic similarity. Concerning (9a) and (9b), we compute $\eta(\tilde{\mathbf{s}}_t, \hat{\tilde{\mathbf{s}}}_t)$ and $\eta(\tilde{\mathbf{s}}_t, \hat{\tilde{\mathbf{s}}}_t^f)$ by deploying the outputs of the sentence Transformer `all-MiniLM-L6-v2` – denoted by $\mathbf{T}_{\Phi}(\cdot)$ – as

$$\eta(\tilde{\mathbf{s}}_t, \hat{\tilde{\mathbf{s}}}_t) = \frac{\mathbf{T}_{\Phi}(\tilde{\mathbf{s}}_t) \cdot \mathbf{T}_{\Phi}(\hat{\tilde{\mathbf{s}}}_t)^T}{\|\mathbf{T}_{\Phi}(\tilde{\mathbf{s}}_t)\| \|\mathbf{T}_{\Phi}(\hat{\tilde{\mathbf{s}}}_t)\|} \quad (10a)$$

$$\eta(\tilde{\mathbf{s}}_t, \hat{\tilde{\mathbf{s}}}_t^f) = \frac{\mathbf{T}_{\Phi}(\tilde{\mathbf{s}}_t) \cdot \mathbf{T}_{\Phi}(\hat{\tilde{\mathbf{s}}}_t^f)^T}{\|\mathbf{T}_{\Phi}(\tilde{\mathbf{s}}_t)\| \|\mathbf{T}_{\Phi}(\hat{\tilde{\mathbf{s}}}_t^f)\|}, \quad (10b)$$

where (10a) and (10b) compute the *cosine similarity* w.r.t. the adopted sentence Transformer's output.

In light of the above-detailed testing setup and assumptions, the prepared testing sentences of Sec. III-C, and the tokenizer of Sec. III-C1, we move on to detail our testing procedures.

B. Testing Procedures

In this subsection, we systematically detail our testing procedures that include mapping an integer to a word, prediction of a recovered sentence, and evaluation of the trained DeepSC models using the metric probability of semantic similarity computed numerically in (9a) and (9b) via (10a) and (10b). We begin with our function that maps an integer to a word.

1) *Mapping an Integer to a Word*: After attempting to learn the probability of each word of a sentence (via `softmax` layers), the relatively wide trained DeepSC model and the relatively wide trained and finetuned DeepSC model return the most likely integer for every word. As every integer except zero encodes a unique word per our employed Keras tokenizer, we implement a Python function that returns a word for a predicted integer. This function accepts an integer index and the tokenizer of Sec. III-C1, and returns a word when a word's index matches the inputted integer index. Otherwise, this function returns nothing.

Appending and joining each word predicted by a trained DeepSC model then produce a recovered sentence, as explained below.

¹²`all-MiniLM-L6-v2` is an important sentence Transformer applicable for semantic similarity estimation and clustering or semantic search [62]. It works by mapping paragraphs and sentences to a 384-dimensional dense vector space [62].

2) *Prediction of a Recovered Sentence*: To determine the recovered sentence of a trained DeepSC model for a given input sentence, a trained DeepSC network should first compute the probability for each word of the input sentence. Based on this probability, we can employ our Keras tokenizer – used in preparing our training, validation, and testing sets (i.e., the tokenizer of Sec. III-C1) – to determine the highly likely word to each tokenized-and-transmitted word. Joining and appending each likely word, one can infer the recovered sentence. Deploying this idea to generate a recovered sequence given the transmitted sequence (source sequence), of words, we wrote a Python function that takes a trained DeepSC model, the tokenizer of Sec. III-C1, and a source sequence of integers (“source”) as its inputs. This function returns the respective recovered sequence by implementing the following steps:

- This function first generates a prediction matrix of size $L \times 22,899$ by using the Keras function and code `model.predict(source)[0]`.
- It then generates the predicted sequence of integers by applying the function `argmax(·)` to every column vector of the already obtained prediction matrix.
- For every predicted integer in a `for` loop, it then generates a word using the function in Sec. V-B1. If the returned word is none, the `for` loop breaks. If not, the `for` loop continues to append each generated word until the last integer’s predicted word is appended and the `for` loop is ended. Upon ending the `for` loop, the function joins the appended words and returns the recovered sentence.

The above-mentioned steps return a recovered sentence for every transmitted testing sentence. Nonetheless, we have 100,000 testing sentences (prepared per Sec. III-C) and the evaluation of our trained DeepSC models needs model update per every testing time slot in case of MI RFI. Model update per each time slot is needed because our considered MI RFI from U Gaussian emitters – per (6a) and (6b) – varies in each time slot. Such time-varying MI RFI has to be accommodated during testing, as detailed below.

3) *Evaluation of the Trained DeepSC Models*: Evaluation of our relatively wide trained DeepSC model and our relatively wide trained and finetuned DeepSC model is carried out using a Python function that we wrote to assess the performance of a trained DeepSC model. This Python function takes a trained DeepSC model, the tokenizer of Sec. III-C1, the testing sequences of Sec. III-C, the corresponding raw Europarl testing sentences, different values of U , K , and L , and returns its computed probability of semantic similarity exhibited by an inputted trained DeepSC model. As this function assesses its fed trained model with and without time-varying MI RFI, its first step is model updating per the possible reception of time-varying MI RFI during testing, as detailed below.

If $U = 0$ (no RFI), the trained DeepSC model evaluation function takes the inputted trained model as an updated model. If $U > 0$, on the other hand, the same function handles the reception of time-varying MI RFI via an MI RFI linear Dense layer that is inserted – per every testing time slot t – to the already trained DeepSC models that are

fed to our model evaluation function. This is accomplished using *three consecutive steps*¹³ that are executed once per every testing time slot t : *i*) trained model disassembling, *ii*) programming and insertion of an MI RFI linear Dense layer, and *iii*) trained model reassembling. Trained model disassembling is accomplished using the following Python code snippet:

```
layers = [l for l in model.layers].
To program an MI RFI linear Dense layer with the magnitude of the  $t$ -th MI RFI that is received w.r.t. a given  $(U, K, L)$  tuple, we first execute the following Python function that computes the  $t$ -th total Gaussian MI RFI received over Rayleigh fading channels.
```

```
def Total_RFI(U, K, L):
    RFI=np.zeros([K*L])
    for j in range(U):
        RFI=RFI+np.random.normal(0, 1, 1)*
math.sqrt(10)*np.random.normal(0, 1, K*L)
    MI_RFI=RFI
    return MI_RFI
```

We then define the t -th *non-trainable* MI RFI linear Dense layer (while exploiting the Keras Dense layer [45]) by employing an identity weight matrix and biases that are equal to the t -th total Gaussian MI RFI vector’s computed values. We then insert this layer into the first Reshape layer’s output of the disassembled trained DeepSC architecture (per Fig. 2) as:

```
MI_RFI_Layer=Dense(K*L, weights =
[np.identity(K*L), Total_RFI(U, K, L)],
activation='linear', trainable=False,
name='MI-RFI_Linear_Dense_Layer')
(layers[5].output).
```

We then reassemble the inputted trained model with the inserted t -th MI RFI linear Dense layer while setting all the constituting layers to be non-trainable as follows:

```
x = MI_RFI_Layer
for i in range(len(layers)):
    layers[i].trainable = False
    if i>5:
        x = layers[i](x).
```

At last, we obtain an updated model – for the t -th testing time slot – via the following code snippet:

```
Updated_model = Model(inputs=layers[0].
input, outputs=x).
```

Once an updated model for the t -th testing time slot is obtained, the trained DeepSC model evaluation function executes the following steps – for every t -th sequence of Sec. III-C’s testing sequences – to compute the exhibited probability of semantic similarity by a given trained DeepSC model:

- First, it generates the t -th recovered sentence using the sentence prediction function of Sec. V-B2.
- Second, it feeds the t -th recovered sentence and the t -th (truncated) raw Europarl testing sentence – truncated to

¹³Since we assumed time-varying MI RFI per (6a) and (6b), we executed trained model disassembling, programming and insertion of an MI RFI linear Dense layer, and trained model reassembling once per every time slot t so as to accommodate any time-varying MI RFI.

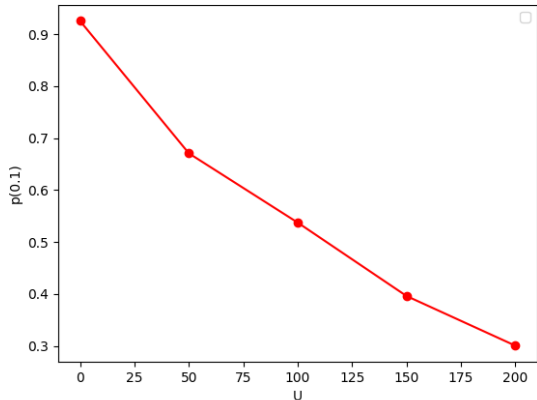


Fig. 10. $p(0.1)$ versus U manifested by our relatively wide trained DeepSC model for $N = 10,000$ testing sentences.

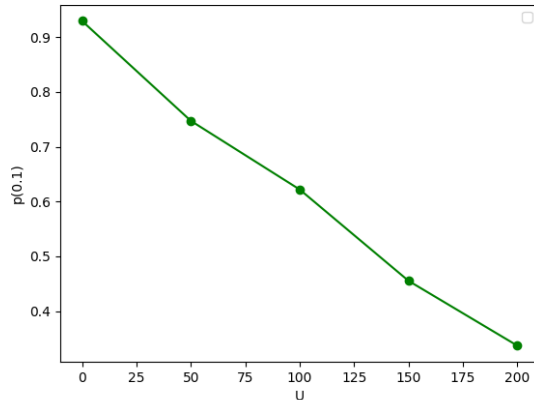


Fig. 11. $p(0.1)$ versus U manifested by our relatively wide trained and finetuned DeepSC model for $N = 10,000$ testing sentences.

length $L = 30$ if $L > 30$ – to the sentence Transformer `all-MiniLM-L6-v2` [62].

- Third, it then feeds the t -th two embedded sentences of `all-MiniLM-L6-v2` to a cosine similarity utility function to compute the t -th semantic similarity value per (10a) or (10b).

Looping over all the aforementioned routines of Sec. V-B3 for N testing time slots, our trained DeepSC model evaluation function finally determines the manifested probability of semantic similarity – by a trained DeepSC model – according to (9a) or (9b).

By inserting the relatively wide trained DeepSC model, the tokenizer of Sec. III-C1, the testing sequences of Sec. III-C, the corresponding raw Europarl testing sentences, different values of U , $K = 8$, and $L = 30$ into the DeepSC model evaluation function of Sec. V-B3, we obtain the t -th relatively wide trained DeepSC model with the t -th MI RFI linear Dense layer of Fig. 16 (see Appendix A) – plotted for $U = 50$ – and the testing results of Sec. V-C1. In addition, we obtain the t -th relatively wide trained and finetuned DeepSC model with the t -th MI RFI linear Dense layer of Fig. 17 (see Appendix A) – plotted for $U = 50$ – and the results reported in Sec. V-C2 by inputting the relatively wide trained and finetuned DeepSC model, the tokenizer of Sec. III-C1, the testing sequences of Sec. III-C, the respective raw Europarl testing sentences, different values of U , $K = 8$, and $L = 30$ into the DeepSC model evaluation function of Sec. V-B3.

C. Testing Results of the Trained DeepSC Models with and without MI RFI

During our testing campaign, we have witnessed many recovered sentences that are surely unrelated with their transmitted counterparts, especially for large U . However, when these semantically unrelated sentences are fed to our adopted sentence Transformer, the resulting sentence embeddings lead to a semantic similarity of around 0.1 (when the embeddings are fed to the cosine similarity utility function). To take this likely limitation – of our adopted sentence transformer – in our probabilistic assessment of semantic irrelevance, we plot

$p(0.1)$ versus U rather than $p(0)$ versus U . The testing results follow.

1) *Testing Results of the Relatively Wide Trained DeepSC Model:* Fig. 10 depicts the $p(0.1)$ versus U plot manifested by our relatively wide trained DeepSC model tested using 10,000 testing sentences. As seen in Fig. 10, our relatively wide trained DeepSC model tends to produce semantically irrelevant sentences as the number of MI RFI interferers becomes large. This trend is consistent with the trend predicted by our recently developed theory.

2) *Testing Results of the Relatively Wide Trained and Finetuned DeepSC Model:* Fig. 11 shows the $p(0.1)$ versus U plot exhibited by our relatively wide trained and finetuned DeepSC model tested using 10,000 testing sentences. This plot also demonstrates that our relatively wide trained and finetuned DeepSC model tends to produce semantically irrelevant sentences as the number of MI RFI interferers gets large, verifying our theory. Meanwhile, comparing Figs. 10 and 11 confirms that our relatively wide trained and finetuned DeepSC model performs slightly better than our relatively wide trained DeepSC model. As expected, this slight training performance improvement is due to finetuning.

3) *Limitations of the Testing Results:* Our recently developed theory predicts that $\lim_{U \rightarrow \infty} p(0) = 0$. However, our testing results – depicted in Figs. 10 and 11 – show that $p(0.1)$ becomes considerably small when U increases. Although this trend was predicted by our recently developed theory [1], the obtained testing results have limitations due to: *i)* the semantic similarity assessment limitation of our adopted sentence Transformer; *ii)* sentence truncation for sequences of sentences that are greater than 30 during training/testing (to alleviate an OOM error we have come across consistently); and *iii)* the training/validation accuracy limit that we have faced repeatedly during our training campaign.

Finally, we draw a conclusion and outline research outlook.

VI. CONCLUDING SUMMARY AND RESEARCH OUTLOOK

This empirical work studied the impact of interference on a text SemCom system dubbed DeepSC. Specifically, we carried

out the training of DeepSC followed by its testing with and without MI RFI using a standard SMT and NMT dataset named Europarl. By employing the training, validation, and testing sets tokenized and vectorized from Europarl, we trained the DeepSC architecture in Keras 2.9 with TensorFlow 2.9 as a backend and then tested it in the presence and absence of Gaussian MI RFI received over Rayleigh fading channels. For this testing setting, the results obtained using our relatively wide trained DeepSC model and the relatively wide trained and finetuned DeepSC model demonstrated that DeepSC tends to produce semantically irrelevant sentences as the number of Gaussian RFI emitters becomes very large, consistent with our recently developed theory on the performance limits of DeepSC under MI RFI [1]. Accordingly, a fundamental 6G design paradigm for IR² SemCom is needed, and our proposed (generic) lifelong DL-based IR² SemCom system [1, Fig. 2] can be an inception.

Informed by interdisciplinary theoretical and empirical research on DL, NLP, NMT, and SemCom, this paper documented extensive details on the steps pertaining to the training of DeepSC and its testing with and without interference. This effectively closes the existing knowledge gap – from an implementation vantage point – that may have already hindered the development of many text SemCom techniques. Consequently, this paper inspires the design and development of numerous text SemCom systems and IR² SemCom systems.

APPENDIX A

THE PARAMETERS AND CONNECTIONS OF DIFFERENT DEEPSC MODELS

For clarity and completeness, this appendix documents the parameters and connections of the narrow DeepSC model and relatively wide DeepSC model. It also documents the t -th relatively wide trained DeepSC model with the t -th MI RFI linear Dense layer and the t -th relatively wide trained and finetuned DeepSC model with the t -th MI RFI linear Dense layer. Particularly, this appendix includes Figs. 13-17:

- Fig. 12 depicts the narrow DeepSC model.
- Fig. 13 tabulates the parameters and connections of the narrow DeepSC model.
- Fig. 14 depicts the relatively wide DeepSC model.
- Fig. 15 tabulates the parameters and connections of the relatively wide DeepSC model.
- Fig. 16 schematizes the t -th relatively wide trained DeepSC model with the t -th MI RFI linear Dense layer that accounts for time-varying MI RFI per (6a).
- Fig. 17 diagrams the t -th relatively wide trained and finetuned DeepSC model with the t -th MI RFI linear Dense layer that takes into account time-varying MI RFI per (6b).

ACKNOWLEDGMENT

The authors acknowledge the Digital Research Alliance of Canada [32] (formerly Compute Canada) for a computational support through the Béluga and Graham GPU clusters.

REFERENCES

- [1] T. M. Getu, W. Saad, G. Kaddoum, and M. Bennis, "Performance limits of a deep learning-enabled text semantic communication under interference," 2023. [Online]. Available: <https://arxiv.org/pdf/2302.14702.pdf>
- [2] Y. LeCun, Y. Bengio, and G. Hinton, "Deep learning," *Nature*, vol. 521, no. 436, pp. 436–444, 2015.
- [3] S. Russel and P. Norvig, *Artificial Intelligence: A Modern Approach*, 3rd ed. Englewood Cliffs, NJ, USA: Prentice Hall, 2018.
- [4] K. He, X. Zhang, S. Ren, and J. Sun, "Deep residual learning for image recognition," in *Proc. CVPR*, 2016, pp. 770–778.
- [5] L. Liu, W. Ouyang, X. Wang, P. Fieguth, J. Chen, X. Liu, and M. Pietikäinen, "Deep learning for generic object detection: A survey," 2019. [Online]. Available: <https://arxiv.org/pdf/1809.02165.pdf>
- [6] G. Hinton, L. Deng, D. Yu, G. E. Dahl, A.-r. Mohamed, N. Jaitly, A. Senior, V. Vanhoucke, P. Nguyen, T. N. Sainath, and B. Kingsbury, "Deep neural networks for acoustic modeling in speech recognition: The shared views of four research groups," *IEEE Signal Process. Mag.*, vol. 29, no. 6, pp. 82–97, 2012.
- [7] A. Torfi, R. A. Shirvani, Y. Keneshloo, N. Tavaf, and E. A. Fox, "Natural language processing advancements by deep learning: A survey," 2020. [Online]. Available: <https://arxiv.org/pdf/2003.01200.pdf>
- [8] T. Young, D. Hazarika, S. Poria, and E. Cambria, "Recent trends in deep learning based natural language processing [review article]," *IEEE Comput. Intell. Mag.*, vol. 13, no. 3, pp. 55–75, 2018.
- [9] F. Stahlberg, "Neural machine translation: A review," *J. Artif. Intell. Res.*, vol. 69, pp. 343–418, 10 2020.
- [10] W. Saad, M. Bennis, and M. Chen, "A vision of 6G wireless systems: Applications, trends, technologies, and open research problems," *IEEE Netw.*, pp. 1–9, 2019.
- [11] C. De Alwis, A. Kalla, Q.-V. Pham, P. Kumar, K. Dev, W.-J. Hwang, and M. Liyanage, "Survey on 6G frontiers: Trends, applications, requirements, technologies and future research," *IEEE Open J. Commun. Soc.*, vol. 2, pp. 836–886, 2021.
- [12] M. Alsabah, M. A. Naser, B. M. Mahmmod, S. H. Abdhussain, M. R. Eissa, A. Al-Baidhani, N. K. Noordin, S. M. Sait, K. A. Al-Utaibi, and F. Hashim, "6G wireless communications networks: A comprehensive survey," *IEEE Access*, vol. 9, pp. 148 191–148 243, 2021.
- [13] K. B. Letaief, W. Chen, Y. Shi, J. Zhang, and Y. A. Zhang, "The roadmap to 6G: AI empowered wireless networks," *IEEE Commun. Mag.*, vol. 57, no. 8, pp. 84–90, Aug. 2019.
- [14] M. Bennis, M. Debbah, and H. V. Poor, "Ultrareliable and low-latency wireless communication: Tail, risk, and scale," *Proc. IEEE*, vol. 106, no. 10, pp. 1834–1853, 2018.
- [15] H. Xie, Z. Qin, G. Y. Li, and B.-H. Juang, "Deep learning enabled semantic communication systems," *IEEE Trans. Signal Process.*, vol. 69, pp. 2663–2675, 2021.
- [16] T. M. Getu, G. Kaddoum, and M. Bennis, "Tutorial-cum-survey on semantic and goal-oriented communication: Research landscape, challenges, and future directions," 2023. [Online]. Available: <https://arxiv.org/pdf/2308.01913.pdf>
- [17] Z. Lu, R. Li, K. Lu, X. Chen, E. Hossain, Z. Zhao, and H. Zhang, "Semantics-empowered communication: A tutorial-cum-survey," 2022. [Online]. Available: <https://arxiv.org/pdf/2212.08487.pdf>
- [18] C. E. Shannon and W. Weaver, *The Mathematical Theory of Communication*. Urbana, IL, USA: Univ. Illinois Press, 1949.
- [19] Z. Weng and Z. Qin, "Semantic communication systems for speech transmission," *IEEE J. Sel. Areas Commun.*, vol. 39, no. 8, pp. 2434–2444, 2021.
- [20] D. Huang, F. Gao, X. Tao, Q. Du, and J. Lu, "Toward semantic communications: Deep learning-based image semantic coding," *IEEE J. Sel. Areas Commun.*, vol. 41, no. 1, pp. 55–71, 2023.
- [21] Y. Huang, B. Bai, Y. Zhu, X. Qiao, X. Su, and P. Zhang, "ISCom: Interest-aware semantic communication scheme for point cloud video streaming," 2022. [Online]. Available: <https://arxiv.org/pdf/2210.06808.pdf>
- [22] T. M. Getu, "Advanced RFI detection, RFI excision, and spectrum sensing: Algorithms and performance analyses." Ph.D. dissertation, Electrical Engineering Department, École de Technologie Supérieure (ÉTS), Montreal, QC, Canada, 2019.
- [23] M. Belkin, D. J. Hsu, S. Ma, and S. Mandal, "Reconciling modern machine-learning practice and the classical bias-variance trade-off," *Proc. Natl. Acad. Sci. U.S.A.*, vol. 116, pp. 15 849–15 854, 2019.
- [24] C. Zhang, S. Bengio, M. Hardt, B. Recht, and O. Vinyals, "Understanding deep learning requires rethinking generalization," 2017. [Online]. Available: <https://arxiv.org/pdf/1611.03530.pdf>
- [25] P. L. Bartlett, A. Montanari, and A. Rakhlin, "Deep learning: a statistical viewpoint," *Acta Numer.*, vol. 30, pp. 87–201, 2021.

- [26] B. Adlam and J. Pennington, "The neural tangent kernel in high dimensions: Triple descent and a multi-scale theory of generalization," 2020. [Online]. Available: <https://arxiv.org/pdf/2008.06786.pdf>
- [27] Q. Hu, G. Zhang, Z. Qin, Y. Cai, G. Yu, and G. Y. Li, "Robust semantic communications against semantic noise," 2022. [Online]. Available: <https://arxiv.org/pdf/2202.03338.pdf>
- [28] Y. E. Sagduyu, T. Erpek, S. Ulukus, and A. Yener, "Is semantic communications secure? a tale of multi-domain adversarial attacks," 2022. [Online]. Available: <https://arxiv.org/pdf/2212.10438.pdf>
- [29] P. Koehn, "European Parliament Proceedings Parallel Corpus 1996-2011," Accessed Jul.-Aug. 2023. [Online]. Available: <https://www.statmt.org/europarl/>
- [30] Keras, "CategoryEncoding layer," Accessed Jul.-Aug. 2023. [Online]. Available: https://keras.io/api/layers/preprocessing_layers/categorical/category_encoding/
- [31] J. Brownlee, "How to Prepare a French-to-English Dataset for Machine Translation," Accessed Jul. 2023. [Online]. Available: <https://machinelearningmastery.com/prepare-french-english-dataset-machine-translation/>
- [32] The Alliance, "Digital Research Alliance of Canada," Accessed Jul.-Aug. 2023. [Online]. Available: <https://alliancecan.ca/en>
- [33] Digital Research Alliance of Canada, "Béluga," Accessed Jul.-Aug. 2023. [Online]. Available: <https://docs.alliancecan.ca/wiki/B%C3%A9luga>
- [34] Digital Research Alliance of Canada, "Graham," Accessed Jul.-Aug. 2023. [Online]. Available: <https://docs.alliancecan.ca/wiki/Graham>
- [35] J. Brownlee, "How to Develop a Neural Machine Translation System from Scratch," Accessed Jul. 2023. [Online]. Available: <https://machinelearningmastery.com/develop-neural-machine-translation-system-keras/>
- [36] TensorFlow, "tf.keras.preprocessing.text.Tokenizer," Accessed Jul.-Aug. 2023. [Online]. Available: https://www.tensorflow.org/api_docs/python/tf/keras/preprocessing/text/Tokenizer
- [37] TensorFlow, "tf.keras.utils.pad_sequences," Accessed Jul.-Aug. 2023. [Online]. Available: https://www.tensorflow.org/api_docs/python/tf/keras/utils/pad_sequences
- [38] TensorFlow, "tf.keras.utils.to_categorical," Accessed Jul.-Aug. 2023. [Online]. Available: https://www.tensorflow.org/api_docs/python/tf/keras/utils/to_categorical
- [39] T. M. Getu, G. Kaddoum, and M. Bennis, "Making sense of meaning: A survey on metrics for semantic and goal-oriented communication," *IEEE Access*, vol. 11, pp. 45 456–45 492, 2023.
- [40] TensorFlow, "tf.keras.utils.sequence," Accessed Jul.-Aug. 2023. [Online]. Available: https://www.tensorflow.org/api_docs/python/tf/keras/utils/Sequence
- [41] Keras, "Model training APIs," Accessed Jul.-Aug. 2023. [Online]. Available: https://keras.io/api/models/model_training_apis/
- [42] Keras, "Adam," Accessed Jul.-Aug. 2023. [Online]. Available: <https://keras.io/api/optimizers/adam/>
- [43] M. I. Belghazi, A. Baratin, S. Rajeswar, S. Ozair, Y. Bengio, A. Courville, and R. D. Hjelm, "MINE: Mutual information neural estimation," 2021. [Online]. Available: <https://arxiv.org/pdf/1801.04062.pdf>
- [44] Keras, "Embedding layer," Accessed Jul.-Aug. 2023. [Online]. Available: https://keras.io/api/layers/core_layers/embedding/
- [45] Keras, "Dense layer," Accessed Jul.-Aug. 2023. [Online]. Available: https://keras.io/api/layers/core_layers/dense/
- [46] A. Vaswani, N. Shazeer, N. Parmar, J. Uszkoreit, L. Jones, A. N. Gomez, L. Kaiser, and I. Polosukhin, "Attention is all you need," 2023. [Online]. Available: <https://arxiv.org/pdf/1706.03762.pdf>
- [47] Keras, "The Model class," Accessed Jul.-Aug. 2023. [Online]. Available: <https://keras.io/api/models/model/>
- [48] Keras, "TransformerEncoder layer," Accessed Jul.-Aug. 2023. [Online]. Available: https://keras.io/api/keras_nlp/modeling_layers/transformer_encoder/
- [49] Keras, "Layer weight initializers," Accessed Jul.-Aug. 2023. [Online]. Available: <https://keras.io/api/layers/initializers/>
- [50] Keras, "SGD," Accessed Jul.-Aug. 2023. [Online]. Available: <https://keras.io/api/optimizers/sgd/>
- [51] Keras, "RMSprop," Accessed Jul.-Aug. 2023. [Online]. Available: <https://keras.io/api/optimizers/rmsprop/>
- [52] F. Chollet, *Deep Learning with Python*. Shelter Island, NY, USA: Manning, 2018.
- [53] Keras, "Reshape layer," Accessed Jul.-Aug. 2023. [Online]. Available: https://keras.io/api/layers/reshaping_layers/reshape/
- [54] T. O'Shea and J. Hoydis, "An introduction to deep learning for the physical layer," *IEEE Trans. Cogn. Commun. Netw.*, vol. 3, no. 4, pp. 563–575, 2017.
- [55] Keras, "TransformerDecoder layer," Accessed Jul.-Aug. 2023. [Online]. Available: https://keras.io/api/keras_nlp/modeling_layers/transformer_decoder/
- [56] T. M. Getu, W. Ajib, and R. Jr. Landry, "Oversampling-based algorithm for efficient RF interference excision in SIMO systems," in *Proc. IEEE Global Conf. on Signal and Inform. Process. (IEEE GlobalSIP)*, Washington DC, DC, USA, Dec. 2016, pp. 1423–1427.
- [57] T. M. Getu, W. Ajib, and O. A. Yeste-Ojeda, "Tensor-based efficient multi-interferer RFI excision algorithms for SIMO systems," *IEEE Trans. Commun.*, vol. 65, no. 7, pp. 3037–3052, Jul. 2017.
- [58] T. M. Getu, W. Ajib, and R. Jr. Landry, "Performance analysis of energy-based RFI detector," *IEEE Trans. Wireless Commun.*, vol. 17, no. 10, pp. 6601–6616, Oct. 2018.
- [59] T. M. Getu, W. Ajib, and R. Jr. Landry, "Power-based broadband RF interference detector for wireless communication systems," *IEEE Wireless Commun. Lett.*, vol. 7, no. 6, pp. 1002–1005, Dec. 2018.
- [60] HuggingFace, "The AI community building the future," Accessed Jul.-Aug. 2023. [Online]. Available: <https://huggingface.co/>
- [61] HuggingFace, "Sentence Transformers," Accessed Jul.-Aug. 2023. [Online]. Available: <https://huggingface.co/sentence-transformers>
- [62] HuggingFace, "sentence-transformers/all-MiniLM-L6-v2," Accessed Jul.-Aug. 2023. [Online]. Available: <https://huggingface.co/sentence-transformers/all-MiniLM-L6-v2>

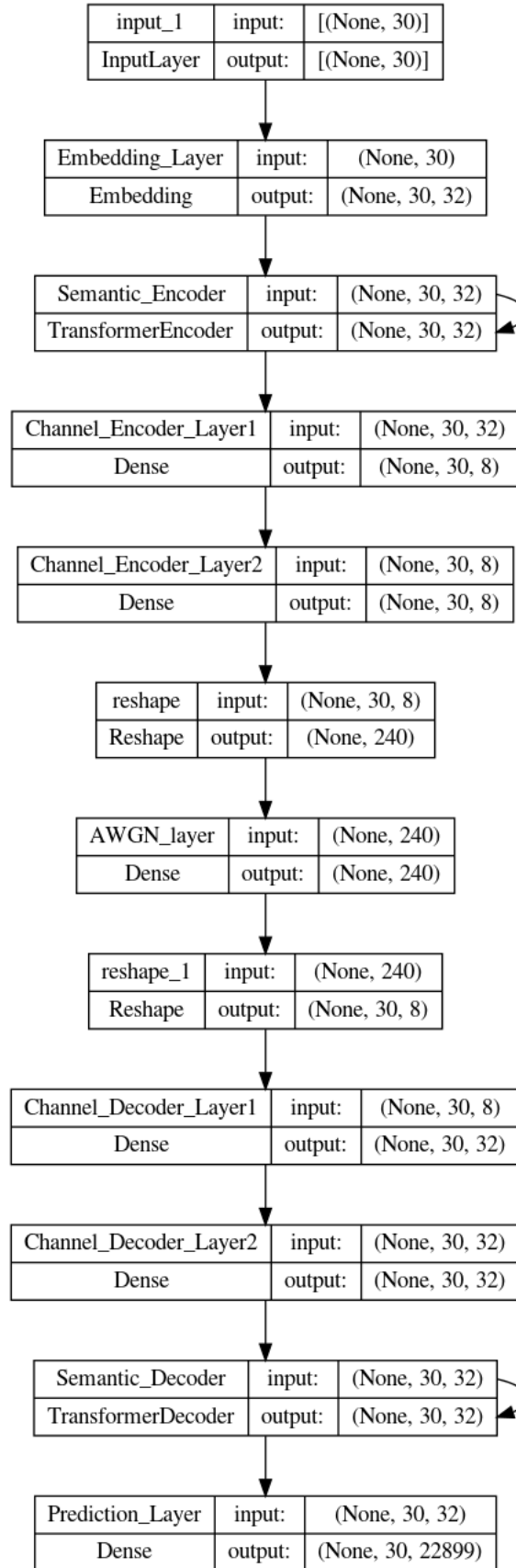


Fig. 12. Narrow DeepSC model: $(K, H, V, E, L) = (8, 10, 32, 32, 30)$.

Layer (type)	Output Shape	Param #	Connected to
input_1 (InputLayer)	[(None, 30)]	0	[]
Embedding_Layer (Embedding)	(None, 30, 32)	960	['input_1[0][0]']
Semantic_Encoder (TransformerEncoder ncoder)	(None, 30, 32)	6202	['Embedding_Layer[0][0]', 'Semantic_Encoder[0][0]', 'Semantic_Encoder[1][0]']
Channel_Encoder_Layer1 (Dense)	(None, 30, 8)	264	['Semantic_Encoder[2][0]']
Channel_Encoder_Layer2 (Dense)	(None, 30, 8)	72	['Channel_Encoder_Layer1[0][0]']
reshape (Reshape)	(None, 240)	0	['Channel_Encoder_Layer2[0][0]']
AWGN_layer (Dense)	(None, 240)	57840	['reshape[0][0]']
reshape_1 (Reshape)	(None, 30, 8)	0	['AWGN_layer[0][0]']
Channel_Decoder_Layer1 (Dense)	(None, 30, 32)	288	['reshape_1[0][0]']
Channel_Decoder_Layer2 (Dense)	(None, 30, 32)	1056	['Channel_Decoder_Layer1[0][0]']
Semantic_Decoder (TransformerDecoder)	(None, 30, 32)	6202	['Channel_Decoder_Layer2[0][0]', 'Semantic_Decoder[0][0]', 'Semantic_Decoder[1][0]']
Prediction_Layer (Dense)	(None, 30, 22899)	755667	['Semantic_Decoder[2][0]']
=====			
Total params: 828,551			
Trainable params: 770,711			
Non-trainable params: 57,840			

Fig. 13. The parameters and connections of narrow DeepSC model.

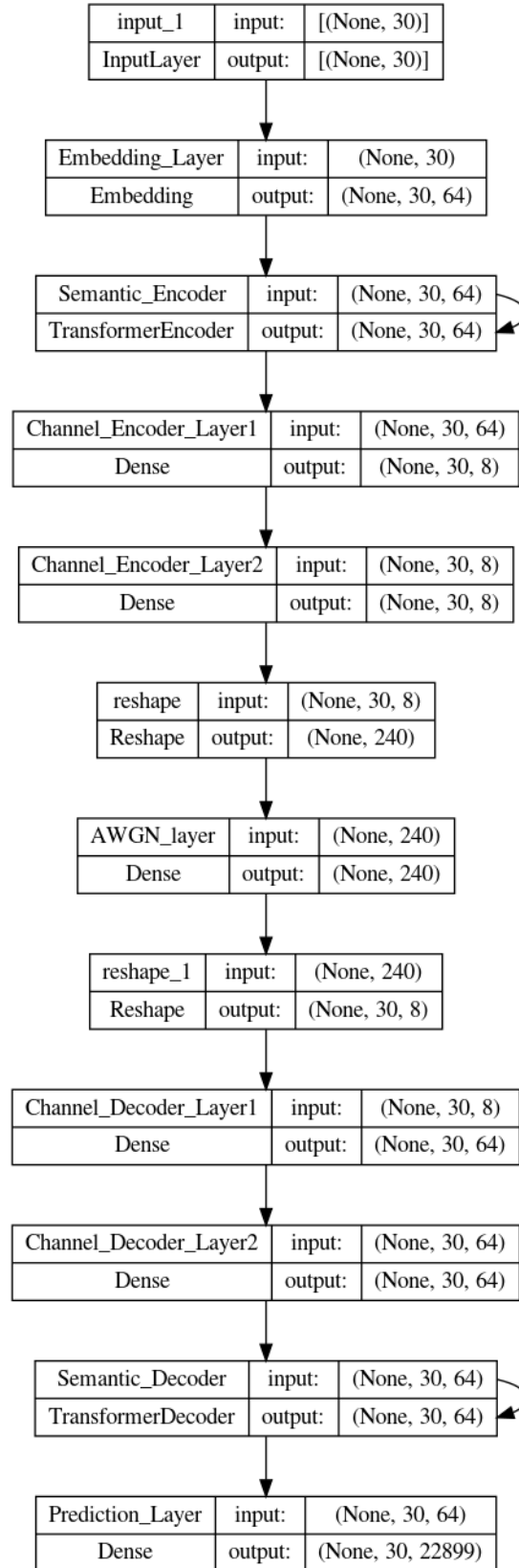


Fig. 14. Relatively wide DeepSC model: $(K, H, V, E, L) = (8, 10, 32, 64, 30)$.

Layer (type)	Output Shape	Param #	Connected to
input_1 (InputLayer)	[(None, 30)]	0	[]
Embedding_Layer (Embedding)	(None, 30, 64)	1920	['input_1[0][0]']
Semantic_Encoder (TransformerEncoder)	(None, 30, 64)	20052	['Embedding_Layer[0][0]', 'Semantic_Encoder[0][0]', 'Semantic_Encoder[1][0]']
Channel_Encoder_Layer1 (Dense)	(None, 30, 8)	520	['Semantic_Encoder[2][0]']
Channel_Encoder_Layer2 (Dense)	(None, 30, 8)	72	['Channel_Encoder_Layer1[0][0]']
reshape (Reshape)	(None, 240)	0	['Channel_Encoder_Layer2[0][0]']
AWGN_layer (Dense)	(None, 240)	57840	['reshape[0][0]']
reshape_1 (Reshape)	(None, 30, 8)	0	['AWGN_layer[0][0]']
Channel_Decoder_Layer1 (Dense)	(None, 30, 64)	576	['reshape_1[0][0]']
Channel_Decoder_Layer2 (Dense)	(None, 30, 64)	4160	['Channel_Decoder_Layer1[0][0]']
Semantic_Decoder (TransformerDecoder)	(None, 30, 64)	20052	['Channel_Decoder_Layer2[0][0]', 'Semantic_Decoder[0][0]', 'Semantic_Decoder[1][0]']
Prediction_Layer (Dense)	(None, 30, 22899)	1488435	['Semantic_Decoder[2][0]']
=====			
Total params: 1,593,627			
Trainable params: 1,535,787			
Non-trainable params: 57,840			

Fig. 15. The parameters and connections of relatively wide DeepSC model.

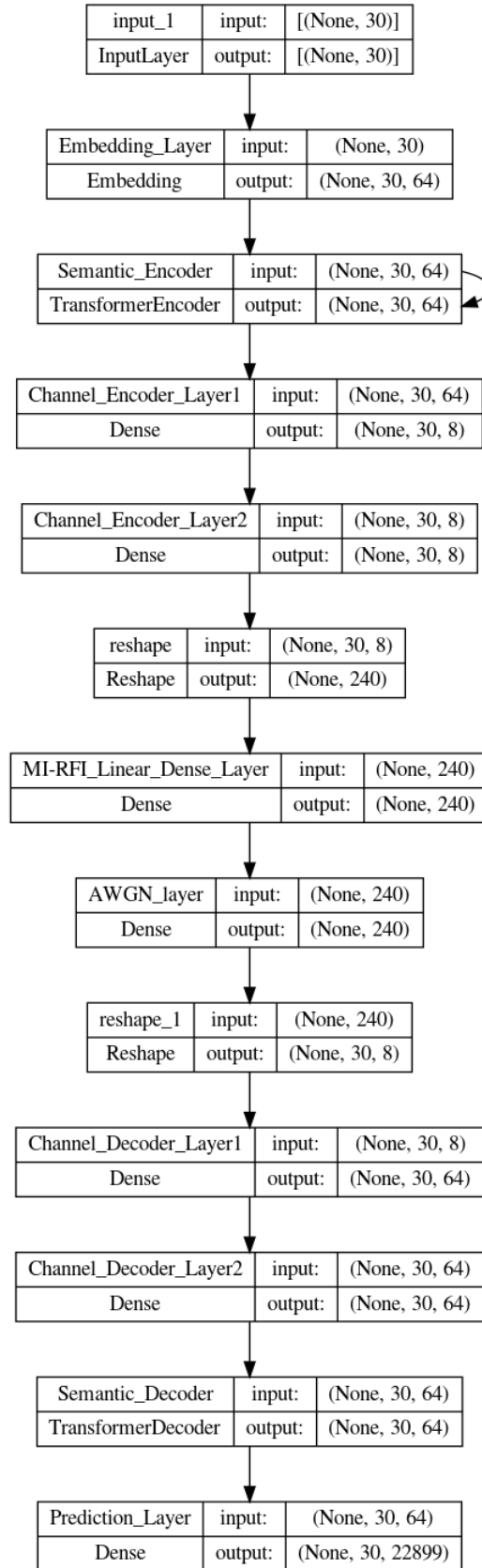


Fig. 16. The t -th relatively wide trained DeepSC model with the t -th MI RFI linear Dense layer that accounts for time-varying MI RFI per (6a).

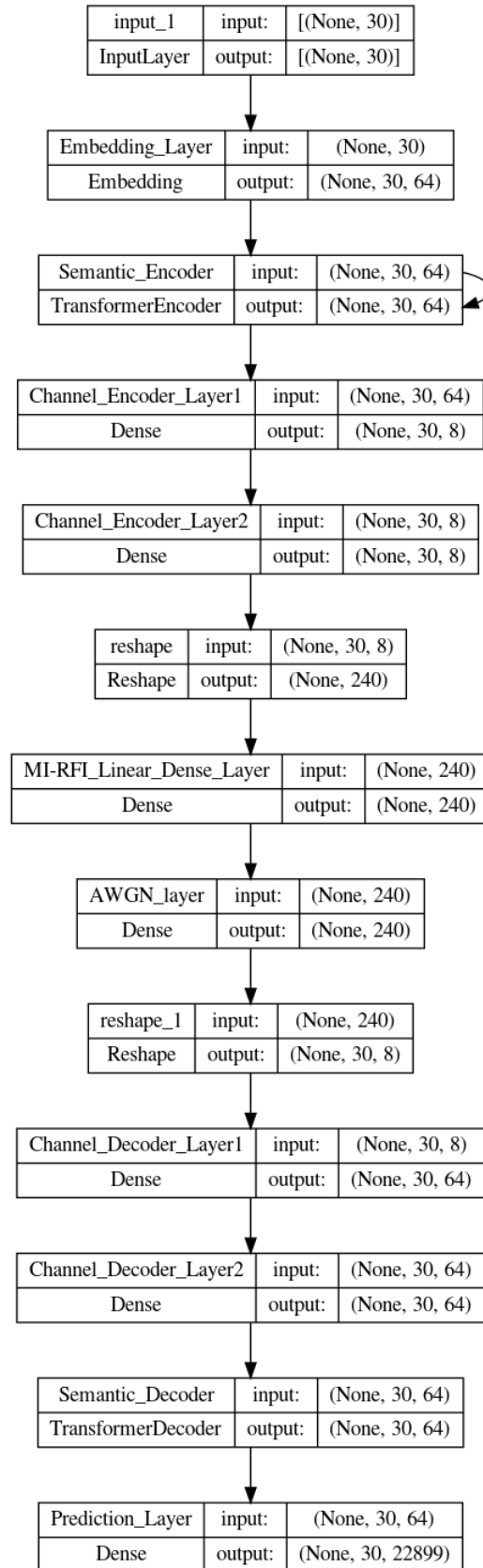


Fig. 17. The t -th relatively wide trained and finetuned DeepSC model with the t -th MI RFI linear Dense layer that takes into account time-varying MI RFI per (6b).